Journal of ELECTRONIC MATERIALS, Vol. 46, No. 5, 2017
DOI: 10.1007/s11664-016-4946-y

Improving Thermoelectric Properties of Nanowires Through Inhomogeneity

J. EDUARDO GONZÁLEZ,[1] VICENTA SÁNCHEZ,[2] and CHUMIN WANG[1,3]

1.—Instituto de Investigaciones en Materiales, Universidad Nacional Autónoma de México, Mexico City, Mexico. 2.—Departamento de Física, Facultad de Ciencias, Universidad Nacional Autónoma de México, Mexico City, Mexico. 3.—e-mail: chumin@unam.mx

Inhomogeneity in nanowires can be present in the cross-section and/or by breaking the translational symmetry along the nanowire. In particular, the quasiperiodicity introduces an unusual class of electronic and phononic transport with a singular continuous eigenvalue spectrum and critically localized wave functions. In this work, the thermoelectricity in periodic and quasiperiodically segmented nanobelts and nanowires is addressed within the Boltzmann formalism by using a real-space renormalization plus convolution method developed for the Kubo–Greenwood formula, in which tight-binding and Born models are, respectively, used for the calculation of electric and lattice thermal conductivities. For periodic nanowires, we observe a maximum of the thermoelectric figure-of-merit (ZT) in the temperature space, as occurred in the carrier concentration space. This maximum ZT can be improved by introducing into nanowires periodically arranged segments and an inhomogeneous cross-section. Finally, the quasiperiodically segmented nanowires reveal an even larger ZT in comparison with the periodic ones.

Key words: Thermoelectricity, Kubo–Greenwood formula, real-space renormalization method, nanowire heterostructures

INTRODUCTION

The direct conversion between thermal and electrical energies by thermoelectric devices has attracted great attention in recent years. Low-dimensional materials seem to be promising candidates for high-performance thermoelectric devices, whose efficiency is determined by the dimensionless figure-of-merit defined as $ZT \equiv (\sigma S^2 T)/(\kappa_{\mathrm{el}} + \kappa_{\mathrm{ph}})$, where the Seebeck coefficient (S), electrical conductivity (σ), electronic (κ_{el}) and phononic (κ_{ph}) thermal conductivities can be calculated by using the Boltzmann formalism.[1] The inherent correlation between these thermoelectric quantities makes difficult to improve the value of ZT.

In general, the Seebeck coefficient (S) is proportional to the average transported electron energy relative to the chemical potential (μ), i.e., $S \propto \langle E - \mu \rangle$.[2] Thus, S is null for μ located at the center of a symmetric electronic band. When μ moves towards the band edges in a three-dimensional system, the magnitude of S grows and σ diminishes. The combination of these two trends leads to the existence of a maximum ZT in the carrier concentration space.[3]

In the temperature space, the power factor (σS^2) is null at zero temperature, since σ or S is, respectively, nil for μ located outside or inside the electronic band. Hence, the power factor increases with T in the low-temperature regime, because it is a positively defined quantity. This trend has been observed in single nanowires.[4,5] For the extreme high-temperature limit, both electrons and holes of a semiconductor have contributions to S with different sign and almost the same magnitude, leading to a significant reduction of the Seebeck coefficient. Consequently, a maximum ZT is often observed in the temperature space.[6]

This maximum ZT can be improved by reducing the cross-section of a nanowire, as reported by many

(Received June 2, 2016; accepted September 7, 2016; published online October 14, 2016)

theoretical[7] and experimental[8] studies, where a rapid growth of the power factor with the reduction of cross-section area is observed. On the other hand, nanowire (NW) heterostructures constitute another important alternative to improve thermoelectric properties, because the phonon scattering at the compositional interfaces leads to a lower lattice thermal conductivity.[9] For example, $M_2O_3(ZnO)_n$ (M = In, Ga, Fe) segmented nanowires reveal the importance of segmentation in nanowires.[10] In fact, a quasiperiodic arrangement of these segments following the Fibonacci sequence could induce interesting changes in the thermoelectric properties of a nanowire, since its energy spectrum is singular continuous on a Cantor set of zero Lebesgue measure[11] whose wavefuctions are critical and self-similarly localized in the real space.[12] In this article, we analyze the dependence of ZT on the temperature, carrier concentration, cross-section area and longitudinal inhomogeneity of a nanowire, by using the Boltzmann and Kubo–Greenwood formalisms and a previously developed renormalization plus convolution method.

In order to isolate the effects of long-range quasiperiodic order on thermoelectric properties, we will carry out this analysis by means of a simple single-electron tight-binding Hamiltonian and a first-neighbor Born model on cubically structured nanowires, without considering the electron–electron and electron–phonon interactions nor the anharmonicity. This kind of electronic Hamiltonians has been successfully used in the description of electronic properties of semiconductors,[13] while its vibrational behavior derived from covalent bonds can be properly reproduced by the nearest-neighbor Born model including central and non-central forces.[14,15] Despite the simplicity of this semi-empirical model, its results can be extended beyond the analyzed parameters, as discussed in "Analysis of Parameter Dependence".

THE MODEL

Based on the Boltzmann formalism and the Kubo–Greenwood formula, thermoelectric quantities can be calculated through[16,17]

$$ZT = \frac{\sigma S^2 T}{\kappa_{\mathrm{el}} + \kappa_{\mathrm{ph}}}, \tag{1}$$

$$\sigma(\mu, T) = e^2 L_0(\mu, T), \tag{2}$$

$$S(\mu, T) = -\frac{L_1(\mu, T)}{|e| T L_0(\mu, T)}, \tag{3}$$

and

$$\kappa_{\mathrm{el}}(\mu, T) = \frac{L_2(\mu, T) L_0(\mu, T) - L_1^2(\mu, T)}{T L_0(\mu, T)}, \tag{4}$$

where

$$L_n(\mu, T) = \frac{-2\hbar}{\pi m^2 \Omega} \int_{-\infty}^{\infty} \mathrm{d}E (E-\mu)^n \frac{\partial f}{\partial E} \mathrm{Tr}\left\{\hat{p}_{\mathrm{x}} \tilde{G}(E) \hat{p}_{\mathrm{x}} \tilde{G}(E)\right\}, \tag{5}$$

being Ω the system volume, $\hat{p}_{\mathrm{x}}$ the projection of momentum operator along the nanowire, $f(E) = \{1 + \exp[(E-\mu)/(k_{\mathrm{B}}T)]\}^{-1}$ the Fermi-Dirac distribution with chemical potential μ and temperature T, $\tilde{G}(E) = G^{+}(E) - G^{-}(E)$ the discontinuity of Green's functions with $G^{+}(E)$ and $G^{-}(E)$ being the retarded and advanced single-electron Green's functions, respectively.[18]

On the other hand, the lattice thermal conductivity (κ_{ph}) can be calculated by using the Kubo–Greenwood formula for phonons given by[19,20]

$$\kappa_{\mathrm{ph}}(T) = \frac{-2\hbar^2}{\pi \Omega k_{\mathrm{B}}} \sum_l \int_0^{\infty} \mathrm{d}\omega \frac{\omega^2 e^{\hbar\omega/k_{\mathrm{B}}T}}{T^2 (e^{\hbar\omega/k_{\mathrm{B}}T} - 1)^2} \mathrm{Tr}\left\{A_{\mathrm{x}} \tilde{G}_{\mathrm{ph}}(\omega) A_{\mathrm{x}} \tilde{G}_{\mathrm{ph}}(\omega)\right\}_l, \tag{6}$$

where the summation of l is over the longitudinal (L) and transversal (T) modes, $\tilde{G}_{\mathrm{ph}}(\omega)$ is the discontinuity of phononic Green's functions determined by $(M\omega^2 I - \Phi) G_{\mathrm{ph}}(\omega) = I$ and the elements of matrix $\mathbf{A}_{\mathrm{x}}$ are $[A_{\mathrm{x}}]_{\nu\nu'}(l,j) \equiv \frac{1}{2}(R_l - R_j)_{\mathrm{x}} \Phi_{\nu\nu'}(l,j)$, being M the atomic mass, $\mathbf{I}$ the matrix identity and $\Phi_{\nu\nu'}(l,j) = \partial^2 V_{lj} / \partial u_{\nu}(l) \partial u_{\nu'}(j)$ the dynamic matrix. The interaction potential (V_{lj}) between nearest-neighbor atoms l and j in the Born model is given by[15] $V_{lj} = \frac{1}{2}(\alpha - \beta)\left|[u(l) - u(j)] \cdot \hat{n}_{lj}\right|^2 + \frac{1}{2}\beta |[u(l) - u(j)]|^2$, where $u(j)$ is the displacement of atom j with respect to its equilibrium position, α and β are the central and non-central restoring force constants, respectively. The unitary vector $\hat{n}_{lj}$ indicates the bond direction between atoms l and j. Notice that in this article the temperature dependence of thermoelectric properties arises from the statistical factors in Eqs. 5 and 6, while the electronic band structure is independent on the carrier concentration determined by the position of chemical potential.

Let us consider a single-band tight-binding Hamiltonian ($\hat{H}$) with null on-site self-energies given by $\hat{H} = \sum_{\langle l,j \rangle} \{t_{l,j} |l\rangle\langle j| + t_{j,l} |j\rangle\langle l|\}$, where $t_{l,j} = t_{j,l}$ is the nearest-neighbor hopping integral. For the sake of simplicity, a uniform bond length (a) is taken and $\hat{p}_{\mathrm{x}} = \frac{im}{\hbar}\left[\hat{H}, x\right] = \frac{ima}{\hbar} \sum_l \{t_{l,l+1} |l\rangle\langle l+1| - t_{l-1,l} |l\rangle\langle l-1|\}$. For a cubically structured nanowire with planar defects, the Hamiltonian $\hat{H}$ and the dynamic matrix Φ are separable, i.e., $\hat{H} = \hat{H}_{\parallel} \otimes \hat{I}_{\perp} + \hat{I}_{\parallel} \otimes \hat{H}_{\perp}$, where $\hat{H}_{\parallel}$ ($\hat{I}_{\parallel}$) and $\hat{H}_{\perp}$ ($\hat{I}_{\perp}$) are Hamiltonians (identity matrices) of the parallel and perpendicular subsystems, respectively. The convolution theorem can be expressed as[21]

$$\mathrm{Tr}\left(\hat{p}_x\tilde{G}(E)\hat{p}_x\tilde{G}(E)\right) = \sum_\lambda \mathrm{Tr}\left(\hat{p}_x\tilde{G}^{\parallel}(E-E_\lambda)\hat{p}_x\tilde{G}^{\parallel}(E-E_\lambda)\right) \quad (7)$$

for electrons and

$$\mathrm{Tr}\left\{A_x\tilde{G}_{\mathrm{ph}}(\omega^2)A_x\tilde{G}_{\mathrm{ph}}(\omega^2)\right\}_l = \sum_\lambda \mathrm{Tr}\left\{A_x\tilde{G}^{\parallel}_{\mathrm{ph}}(\omega^2-\omega_\lambda^2)A_x\tilde{G}^{\parallel}_{\mathrm{ph}}(\omega^2-\omega_\lambda^2)\right\}_l \quad (8)$$

for phonons, where E_λ and $M\omega_\lambda^2$ are eigenvalues of $\hat{H}_\perp$ and $\Phi_\perp$, respectively. In this article, we only analyze the bond problem, i.e., nanowires with null self-energies and a constant atomic mass (M).

PERIODIC NANOWIRES

For cubically structured periodic NW of $N_\parallel N_\perp$ atoms connected to two semi-infinite periodic NW leads with hopping integrals t and Born central (α) and non-central (β) interactions, analytical solutions of thermoelectric quantities can be found, since the traces of Eqs. 7 and 8 for a periodic NW with square cross-section of $N_\perp$ atoms are, respectively, given by,[22]

$$\mathrm{Tr}\left\{\hat{p}_x\tilde{G}(E)\hat{p}_x\tilde{G}(E)\right\} = \sum_\lambda \left[\Theta(E-E_\lambda+2|t|)-\Theta(E-E_\lambda-2|t|)\right] (N_\parallel-1)^2a^2m^2\Big/\left(2\hbar^2\right) \quad (9)$$

and

$$\mathrm{Tr}\left\{A_x\tilde{G}_{\mathrm{ph}}(\omega^2)A_x\tilde{G}_{\mathrm{ph}}(\omega^2)\right\}_l = -\sum_\lambda\left[\left[1-\Theta\left(\omega^2-\omega_{\lambda_l}^2-4\omega_l^2\right)\right](N_\parallel-1)^2a^2\Big/8\right], \quad (10)$$

where $\Theta(x)$ is the Heaviside step function, ω_l^2 could be $\omega_\alpha^2=\alpha/M$ for longitudinal or $\omega_\beta^2=\beta/M$ for transversal vibrational modes,

$$E_\lambda = -2|t|\left\{\cos\left[m\pi\Big/\left(N_\perp^{1/2}+1\right)\right]+\cos\left[n\pi\Big/\left(N_\perp^{1/2}+1\right)\right]\right\}, \quad (11)$$

$$\omega_{\lambda_{\mathrm{L}}}^2 = 2\omega_\beta^2\left\{2-\cos\left[(m-1)\pi\Big/N_\perp^{1/2}\right]-\cos\left[(n-1)\pi\Big/N_\perp^{1/2}\right]\right\}, \quad (12)$$

and

$$\omega_{\lambda_{\mathrm{T}}}^2 = 2\omega_\alpha^2\left\{1-\cos\left[(m-1)\pi\Big/N_\perp^{1/2}\right]\right\}+2\omega_\beta^2\left\{1-\cos\left[(n-1)\pi\Big/N_\perp^{1/2}\right]\right\}, \quad (13)$$

being $m=1,2,\ldots,N_\perp^{1/2}$ and $n=1,2,\ldots,N_\perp^{1/2}$.

In Fig. 1, we show (a–d) the electronic density of states $\mathrm{DOS}(\mu)=-\frac{1}{\pi}\sum_j \mathrm{Im}\left[G_j^+(\mu)\right]$ (blue lines) and (a′–d′) the zero-temperature electrical conductance $g(\mu)=\sigma(\mu)\Omega_\perp/\Omega_\parallel$ (red lines) normalized by the quantum conductance $g_0=2e^2/h$ as functions of the chemical potential (μ) for (a,a′) a periodic chain, (b,b′) a periodic nanobelt with cross-section of 7×1 atoms, and periodic nanowires with cross-sections of (c,c′) 7×3 and (d,d′) 7×5 atoms, whose structures are schematically presented in the respective figures (a″–d″). All these nanostructures have a length of $N_\parallel=100663297$ atoms connected to two semi-infinite periodic leads with the same cross-section and Hamiltonian parameters of the system. The figures of this section correspond to periodic nanostructures with null self-energies, hopping integral $t=-1$ eV, atomic mass $M=4.81381\times10^{-26}$ kg, central and non-central restoring force constants $\alpha=100$ N/m and $\beta=20$ N/m, respectively. These vibrational parameters are close to those of crystalline silicon[15] and lead to $\hbar\omega_\alpha=30$ meV. The imaginary part of energy used in this article has been $\eta=10^{-3}|t|$ for DOS and $\eta=10^{-3}|t|/N_\parallel$ for conductance. Observe the quantized conductance steps present in these periodic nanostructures and its number grows with the cross-section area. Furthermore, in DOS spectra, the van Hove singularity is found at the edge of each step.

In Fig. 2, we show (a, a′, a″) the density of states (DOS) (gray lines) and electrical conductivity (σ) normalized by $\sigma_0=e^2\Omega_\parallel/(a\pi\hbar)$ of a periodic chain, (b, b′, b″) Seebeck coefficient (S) normalized by $S_0=-k_B/|e|$, (c, c′, c″) thermal conductivity by electrons (κ_{el}), (d, d′, d″) lattice thermal conductivity (κ_{ph}) normalized by $\kappa_0=k_B\omega_\alpha\Omega_\parallel/(2a\pi)$ of a periodic chain, and (e, e′, e″) ZT as functions of chemical potential (μ) for the same periodic (a–e) nanobelt, (a′–e′) nanowire with cross-section of 7×3 atoms and (a″–e″) nanowire with cross-section of 7×5 atoms as in Fig. 1. The temperature (T) dependence of these thermoelectric properties is exhibited in Fig. 3 for the same nanostructures analyzed in Fig. 2, where the chemical potentials are chosen at $\mu_{\mathrm{out}}=E_c-0.01$ eV and $\mu_{\mathrm{in}}=E_c-0.01$ eV, being band edges at $E_c=-3.84776$ eV, $E_c=-5.26197$ eV and $E_c=-5.57981$ eV, respectively, for the periodic nanobelt with cross-section of 7×1, and nanowires with cross-sections of 7×3 and 7×5 atoms.

Observe that the electrical (σ) and thermal conductivities (κ_{el} and κ_{ph}) in Fig. 2 diminish with the growth of cross-section area, due to the quantum interference between conduction channels. For a given temperature, the Seebeck coefficient (S) linearly increases when μ moves away from the band edge and this linear dependence has a weak influence of the cross-section area. Furthermore, maximum values of ZT are found, as a consequence of the growth of σ and the decay of S when μ increases, and

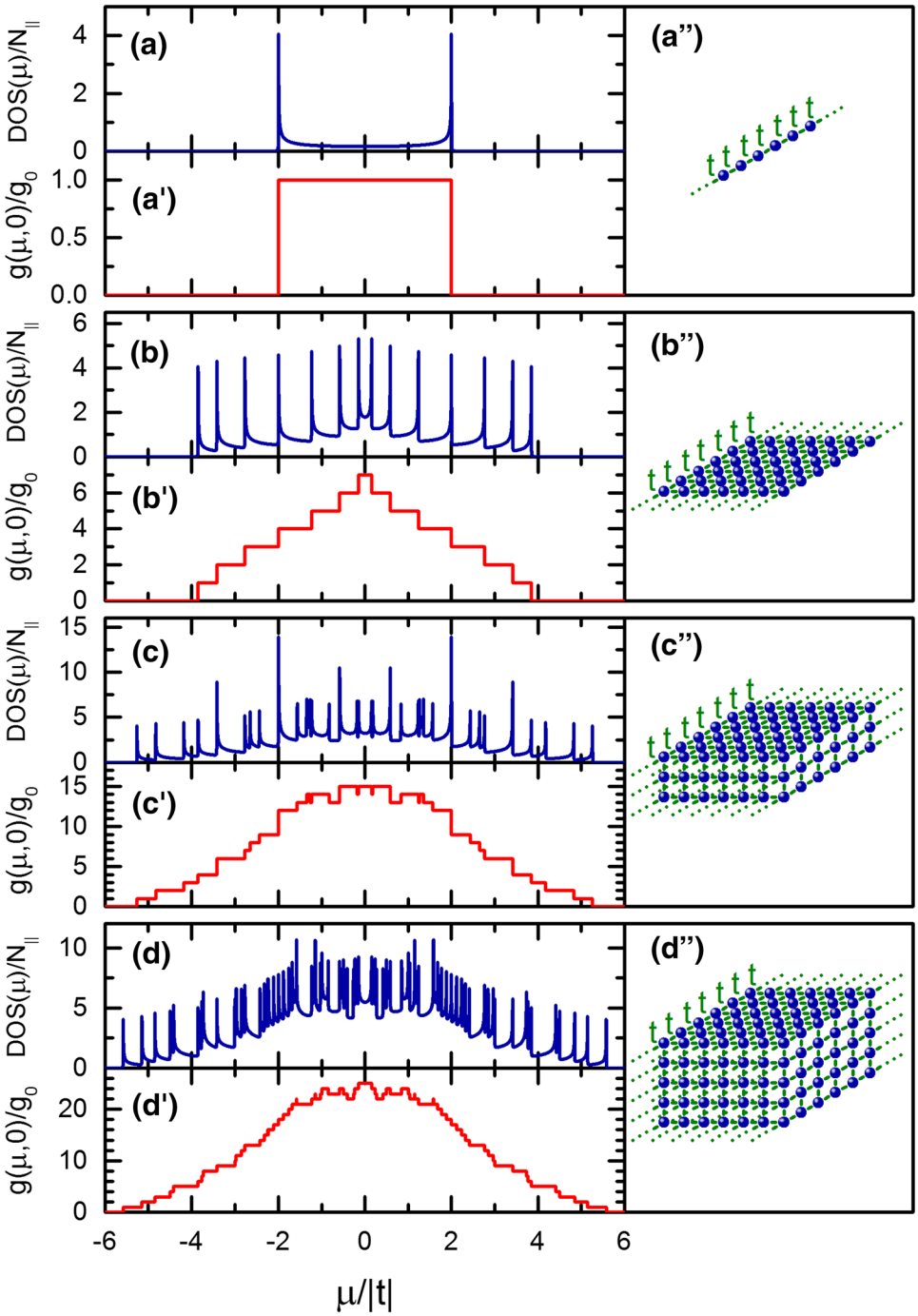

Fig. 1. (a–d) Density of states (DOS) (blue lines) and (a′–d′) zero-temperature electrical conductance (g) (red lines) as functions of chemical potential (μ) for (a, a′) a periodic chain, (b, b′) a periodic nanobelt, and periodic nanowires with cross-sections of (c, c′) 7 × 3 and (d, d′) 7 × 5 atoms, whose structure sketches are, respectively, shown in (a″–d″) (Color figure online).

their locations go away from the band edge when the temperature increases.

Figure 3 exhibit thermoelectric properties obtained from the same nanobelt and nanowires of Fig. 2, now versus the temperature (T). Observe the metallic (blue triangles) and semiconducting (magenta circles) behaviors of the electrical conductivity (σ), when the chemical potential (μ) is, respectively, placed inside ($\mu_{\text{in}} = E_{\text{c}} + 0.01|t|$) and outside ($\mu_{\text{out}} = E_{\text{c}} - 0.01|t|$) the electronic band. In fact, the thermal conductivity by electrons (κ_{el}) is related to σ through the Wiedemann-Franz law given by $\kappa_{\text{el}} = \pi^2 k_{\text{B}}^2 \sigma T/(3e^2)$ when $\mu = \mu_{\text{in}}$. Furthermore, the thermal conductivity by phonons (κ_{ph})

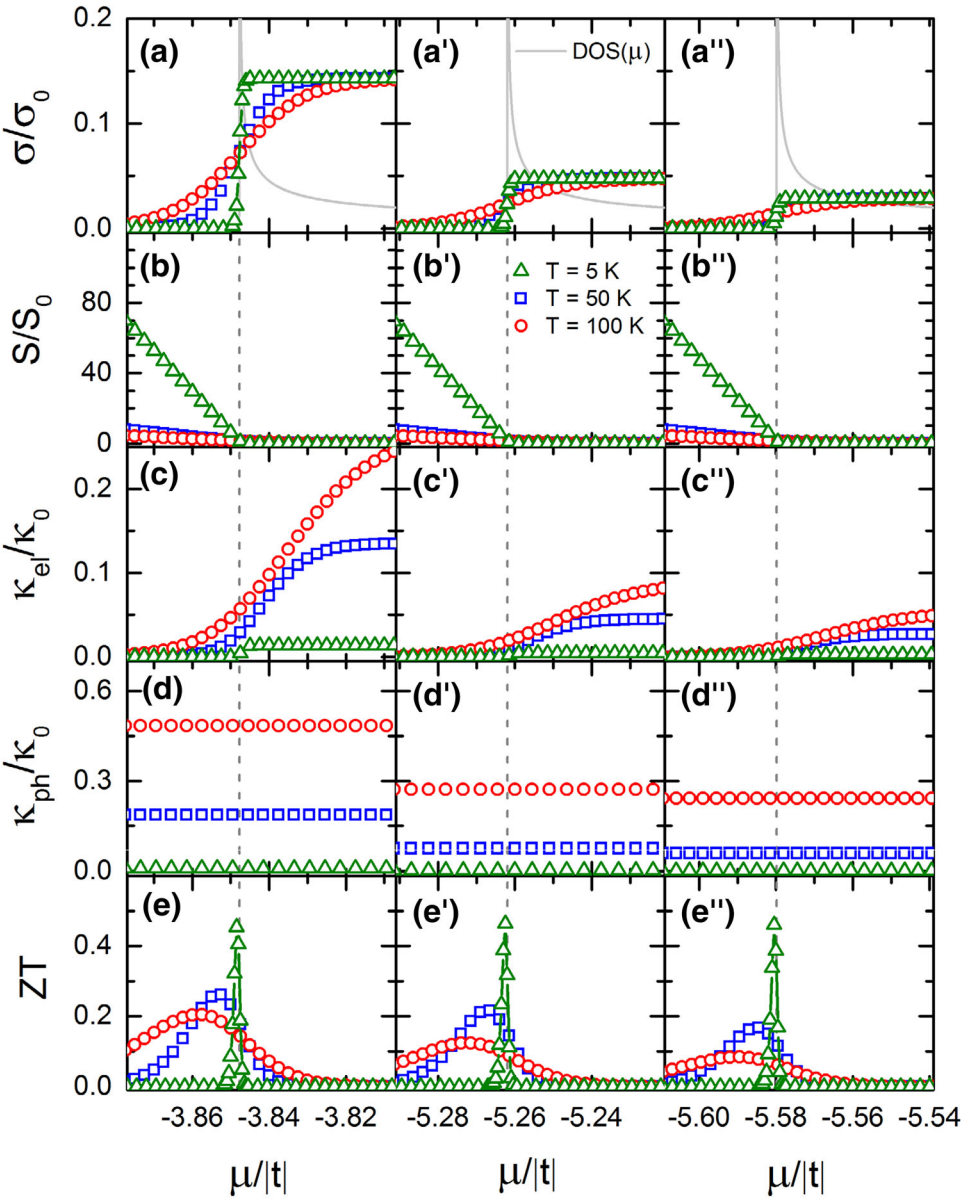

Fig. 2. (a, a′, a″) Density of states (DOS) and electrical conductivity (σ), (b, b′, b″) Seebeck coefficient (S), (c, c′, c″) thermal conductivity by electrons (κ_{el}), (d, d′, d″) thermal conductivity by phonons (κ_{ph}), and (e, e′, e″) figure-of-merit (ZT) as functions of chemical potential (μ) for periodic nanobelt and nanowires with cross-sections of (a–e) 7 × 1, (a′–e′) 7 × 3, and (a″–e″) 7 × 5 atoms.

grows with T, the Seebeck coefficient (S) decreases with T, and the maxima of ZT in the temperature space diminish with the growth of cross-section area, when $\mu = \mu_{out}$.

SEGMENTED NANOWIRES

In this section, we study segmented nanobelts and nanowires with two types of blocks, A and B, which can be periodic or quasiperiodically arranged, as respectively shown in Fig. 4a–d and a′–d′. For the quasiperiodic case, these blocks are ordered following the Fibonacci sequence (F) defined by the addition rule given by $F(n) = F(n-1) \oplus F(n-2)$, where n is the generation number and $\oplus$ indicates the catenation process. If $F(1) = A$ and $F(2) = AB$, the Fibonacci chain of generation four is $F(4) = ABAAB$.

For this study, we chose blocks of three bonds, which can be characterized by hopping integrals (t_A, t_B) or by central (α_A, α_B) and non-central (β_A, β_B) restoring force constants, when the electronic or phononic transport is addressed. The studied nanobelts and nanowires have inhomogeneous cross-sections with non-constant hopping integrals (t_n^x and t_n^y) placed in such a way that maintains the mirror

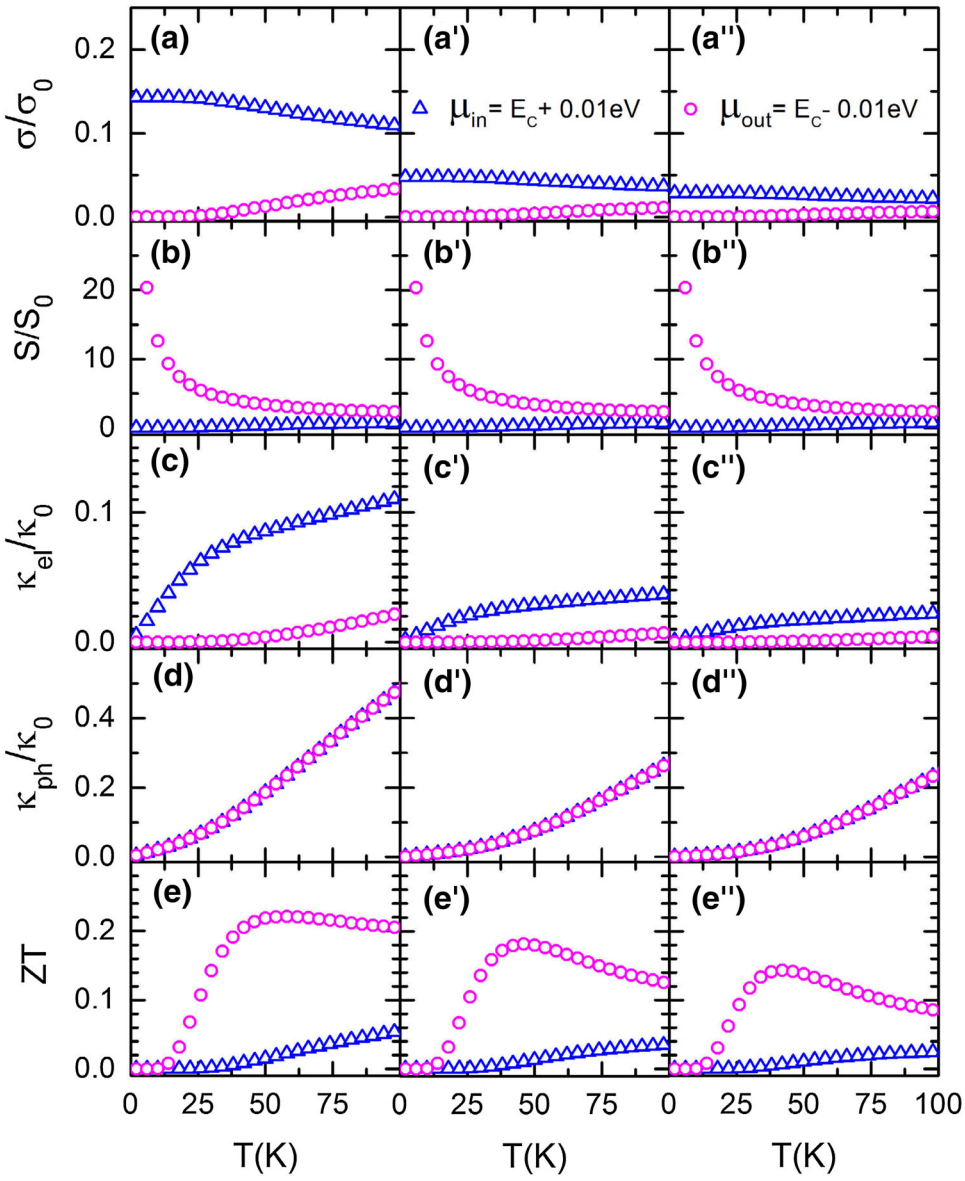

Fig. 3. Temperature (T) dependence of (a, a′, a″) electrical conductivity (σ), (b, b′, b″) Seebeck coefficient (S), (c, c′, c″) thermal conductivity by electrons (κ_{el}), (d, d′, d″) thermal conductivity by phonons (κ_{ph}), and (e, e′, e″) figure-of-merit (ZT) for periodic nanobelt and nanowires with cross-sections of (a–e) 7 × 1, (a′–e′) 7 × 3, and (a″–e″) 7 × 5 atoms.

symmetry along both x and y directions, as illustrated in Fig. 4.

Figure 5 shows the electronic density of states (DOS) (blue lines) and the zero-temperature electrical conductance (g) (red lines) versus the chemical potential (μ) for (a–d) periodically and (a′–d′) quasiperiodically segmented (a, a′) single chains, (b, b′) nanobelts with cross-section of 7 × 1 atoms, and nanowires with cross-sections of (c, c′) 7 × 3 and (d, d′) 7 × 5 atoms, whose atomic ordering is sketched in Fig. 4. The numerical calculations were performed by taking $t_A = 0.3t$, $t_B = t$, $\alpha_A = 0.3\alpha$, $\alpha_B = \alpha$, $\beta_A = 0.3\beta$, $\beta_B = \beta$ and a uniform atomic mass $M = 4.81381 \times 10^{-26}$ kg, where $t = -1$ eV is the hopping integral, $\alpha = 100$ N/m and $\beta = 20$ N/m are, respectively, central and non-central restoring force constants of the periodic leads.

The analyzed nanobelts and nanowires in Fig. 5 have a inhomogeneous cross-section, whose atoms are connected by hopping integrals $t_j^v = c_j^v t$, central $\alpha_j^v = c_j^v \alpha$ and non-central $\beta_j^v = c_j^v \beta$ restoring force constants, where $j = 1$, 2, or 3 and $v = x$ or y with $c_1^x = 1.249$, $c_2^x = 0.855$, $c_3^x = 0.579$, $c_1^y = 0.365$, $c_2^y = 0.517$, and $c_3^y = 0.632$. The periodically segmented nanostructures have a length of $N_{\|} = 100663297$ atoms and quasiperiodic ones have a length of $N_{\|} = 117264509$ atoms corresponding to generation $n = 36$. Notice the multiband structure in Fig. 5a–d, which are related to the periodic

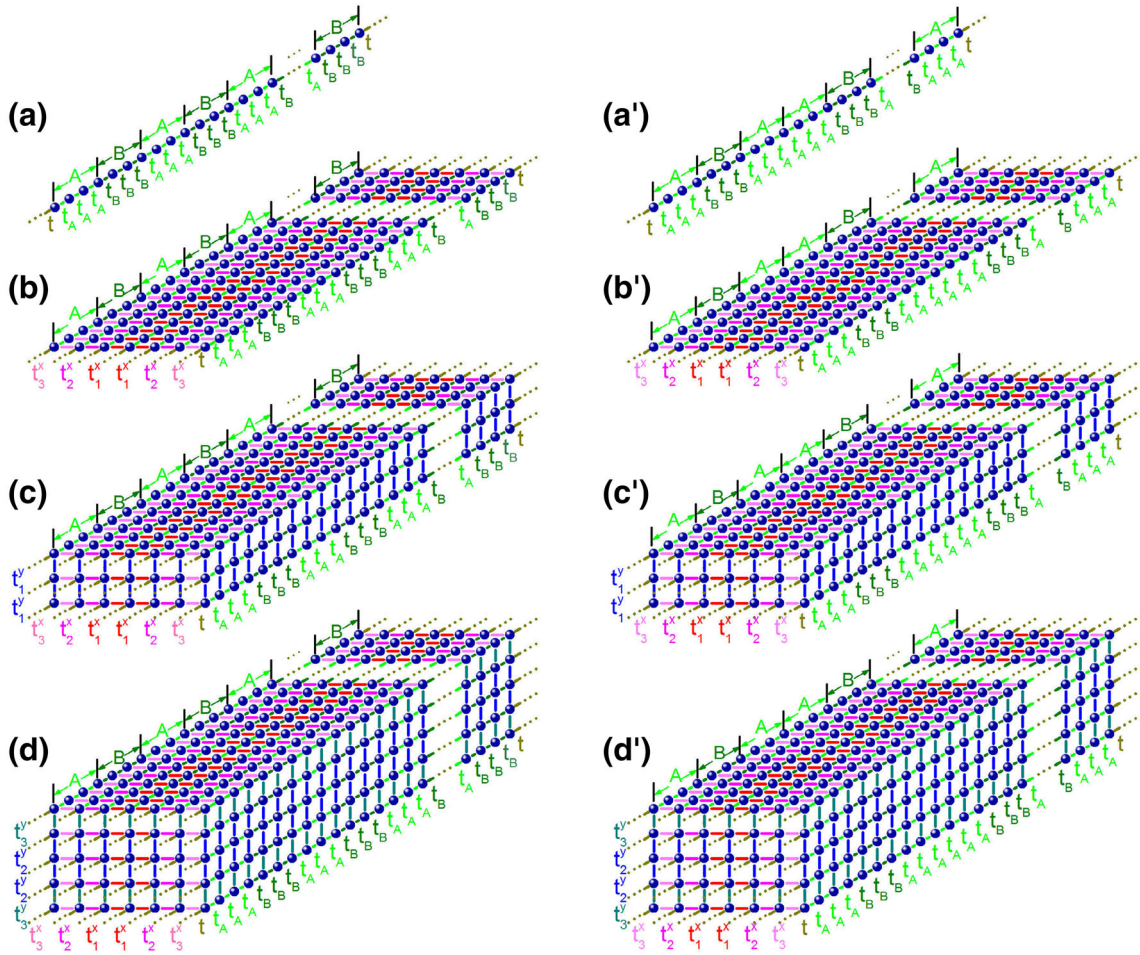

Fig. 4. Schematic representation of (a–d) periodic and (a′–d′) quasiperiodically segmented nanostructures, being (a, a′) single chains, (b, b′) nanobelts with cross-section of 7×1 atoms, (c, c′) and (d, d′) nanowires with cross-sections of 7×3 and 7×5 atoms, respectively. Both segments, *A* and *B*, contain three bonds characterized by hopping integrals t_A or t_B. The cross-sections have non-constant hopping integrals distributed by keeping the mirror symmetry.

segmentation. For example, there are six electronic bands in Fig. 5a, which is originated by folding the first Brillouin zone of a non-segmented linear chain with a new lattice constant $\tilde{a} = 6a$.[23] Moreover, the values of hopping integral in the cross-section were chosen in order to preserve true band gaps around the spectrum center ($\mu = 0$) in Fig. 5b–d. For the quasiperiodic case, at the spectrum center of Fig. 5a′ there is a narrow band containing a transparent state[24] surrounded by two band gaps, and such feature is almost preserved in Fig. 5b′–d′. In general, the conductance peaks of quasiperiodic systems are smaller than those of periodic ones, due to the absence of translational symmetry. However, this reduction of electrical conductance does not necessarily imply a worse thermoelectric efficiency.

In Fig. 6, we show (a, a′, a″) the density of states (DOS) (gray lines) and electrical conductivity (σ), (b, b′, b″) Seebeck coefficient (S), (c, c′, c″) thermal conductivity by electrons (κ_{el}), (d, d′, d″) lattice thermal conductivity (κ_{ph}), and (e, e′, e″) ZT as functions of chemical potential (μ) for the same periodically segmented (a–e) nanobelts and nanowires with cross-sections of (a′–e′) 7 × 3 and (a″–e″) 7 × 5 atoms as in Fig. 5, at temperatures of 5 K (green triangles), 50 K (blue squares) and 100 K (red circles). The dashed lines in these figures indicate the electronic band edges.

Notice that in Fig. 6 the values of σ, S and κ_{el} are unchanged when the cross-section area grows, in contrast to the clear reduction of κ_{ph}, as occurred in Fig. 2a–a″, c–c″ and d–d″ for periodic nanobelts and nanowires without segmentation. These collective behavior leads to an increase of the maximum values of ZT when the cross-section area goes up. These maxima are located out of the electronic band and approach to the band edge located at $E_c = -0.348652$ eV when the temperature diminishes.

Figure 7 exhibit the thermoelectric properties versus temperature (T) for the same nanobelts and nanowires analyzed in Fig. 6. The chemical

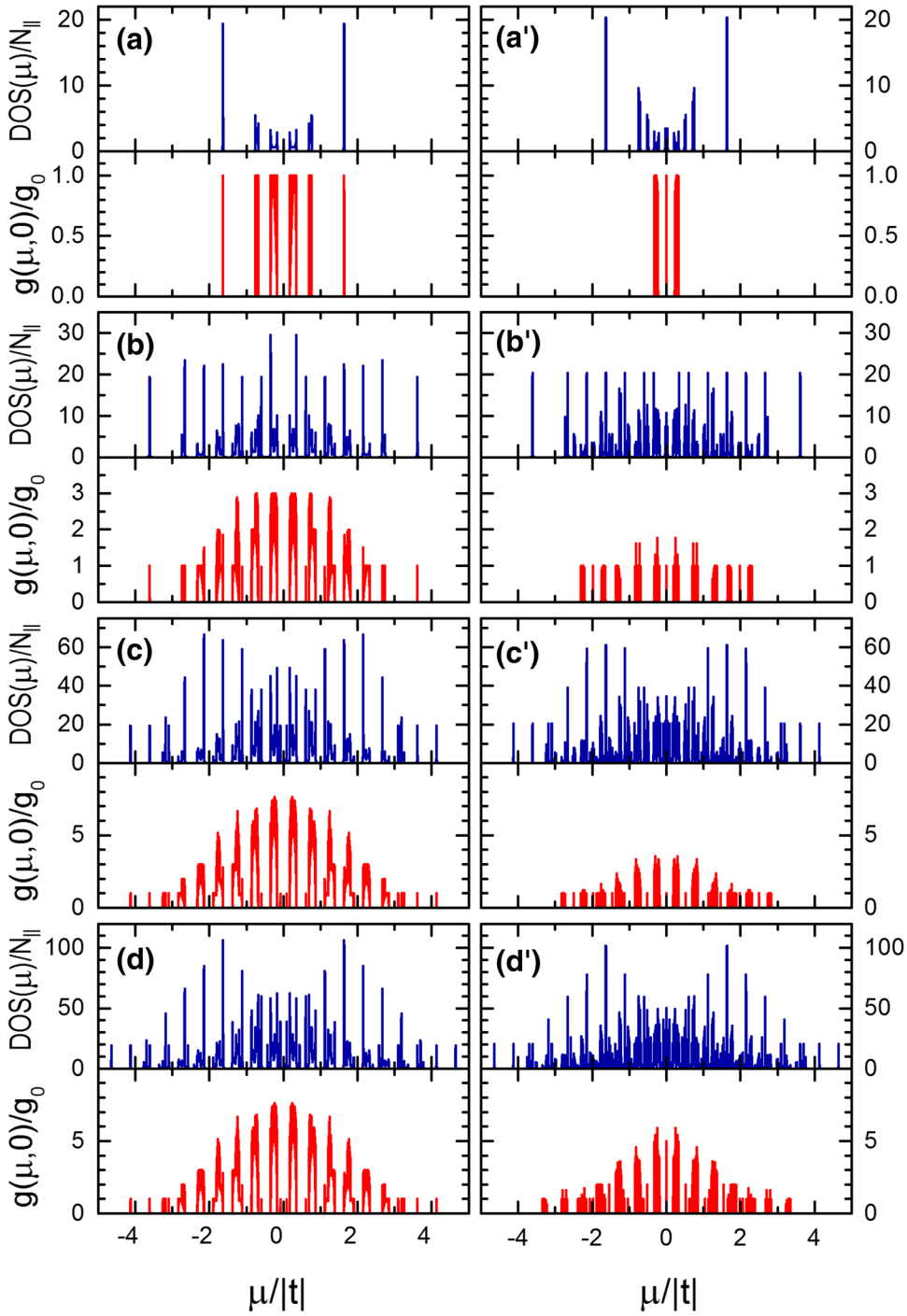

Fig. 5. Density of states (DOS) (blue lines) and zero-temperature electrical conductance (g) (red lines) versus chemical potential (μ) for (a–d) periodic and (a′–d′) quasiperiodically segmented (a, a′) single chains, (b, b′) nanobelts with a cross-section of 7 × 1 atoms, and nanowires with cross-sections of (c, c′) 7 × 3 and (d, d′) 7 × 5 atoms (Color figure online).

potentials (μ) were chosen for $\mu_{in} = E_c + 0.01$ eV (blue triangles) and $\mu_{out} = E_c + 0.01$ eV (magenta circles) for the same band edge of Fig. 6. Notice the growth of ZT from 0.2 of Fig. 3 to almost unity and its enhancement with the cross-section area, when the segmentation and inhomogeneous cross-section are introduced, in spite of the qualitative likeness between Figs. 3 and 7.

In Fig. 8, the same thermoelectric properties of Fig. 6 are exhibited as functions of the chemical potential (μ) for quasiperiodically segmented (a–e) nanobelts and nanowires with cross-sections of (a′–e′) 7 × 3 and (a″–e″) 7 × 5 atoms sketched in Fig. 4b′–d′. The analyzed band edge is located at $E_c = -0.33234$ eV. Observe the fluctuation of the electrical conductivity (σ) at 5 K around

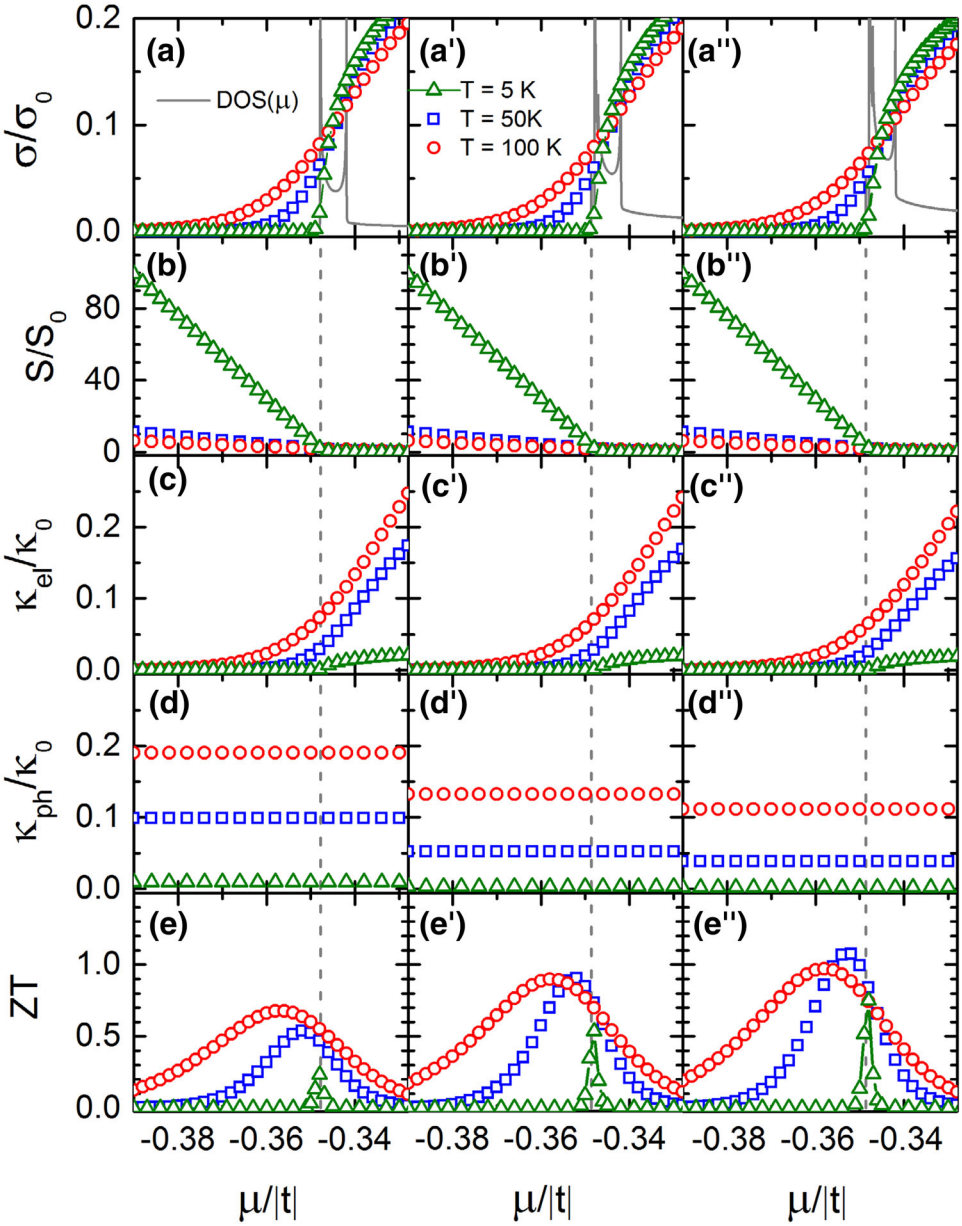

Fig. 6. (a, a′, a″) Density of states (DOS) and electrical conductivity (σ), (b, b′, b″) Seebeck coefficient (S), thermal conductivities by (c, c′, c″) electrons (κ_{el}) and (d, d′, d″) phonons (κ_{ph}), and (e, e′, e″) figure-of-merit (ZT) as functions of chemical potential (μ) for periodically segmented nanobelts and nanowires with inhomogeneous cross-sections of (a–e) 7 × 1, (a′–e′) 7 × 3, and (a″–e″) 7 × 5 atoms.

$\mu = -0.32$ eV, consistent with the density of states spectra (solid gray lines). These fluctuations caused by a dense distribution of bands and gaps smooth out as the temperature grows. Moreover, we note an additional increase of 20% in the maximum ZT at 100 K, mainly due to the reduction of thermal conductivities.

Figure 9 show the temperature dependence of thermoelectric properties corresponding to quasiperiodically segmented nanostructures of Fig. 8. The analyzed chemical potentials (μ) were $\mu_{in} = E_c + 0.01$ eV (blue triangles) and $\mu_{out} = E_c - 0.01$ eV (magenta circles) with $E_c = -0.33234$ eV. In contrast to Fig. 7, ZT for μ_{in} is close to that for μ_{out}, raised from a neither metallic nor semiconductor temperature dependence of σ. Also, we observe an almost linear growth of ZT with temperature around 100 K, which suggests a possible larger ZT close to the room temperature.

ANALYSIS OF PARAMETER DEPENDENCE

There are essentially four parameters in the electronic and vibrational Hamiltonians of periodic

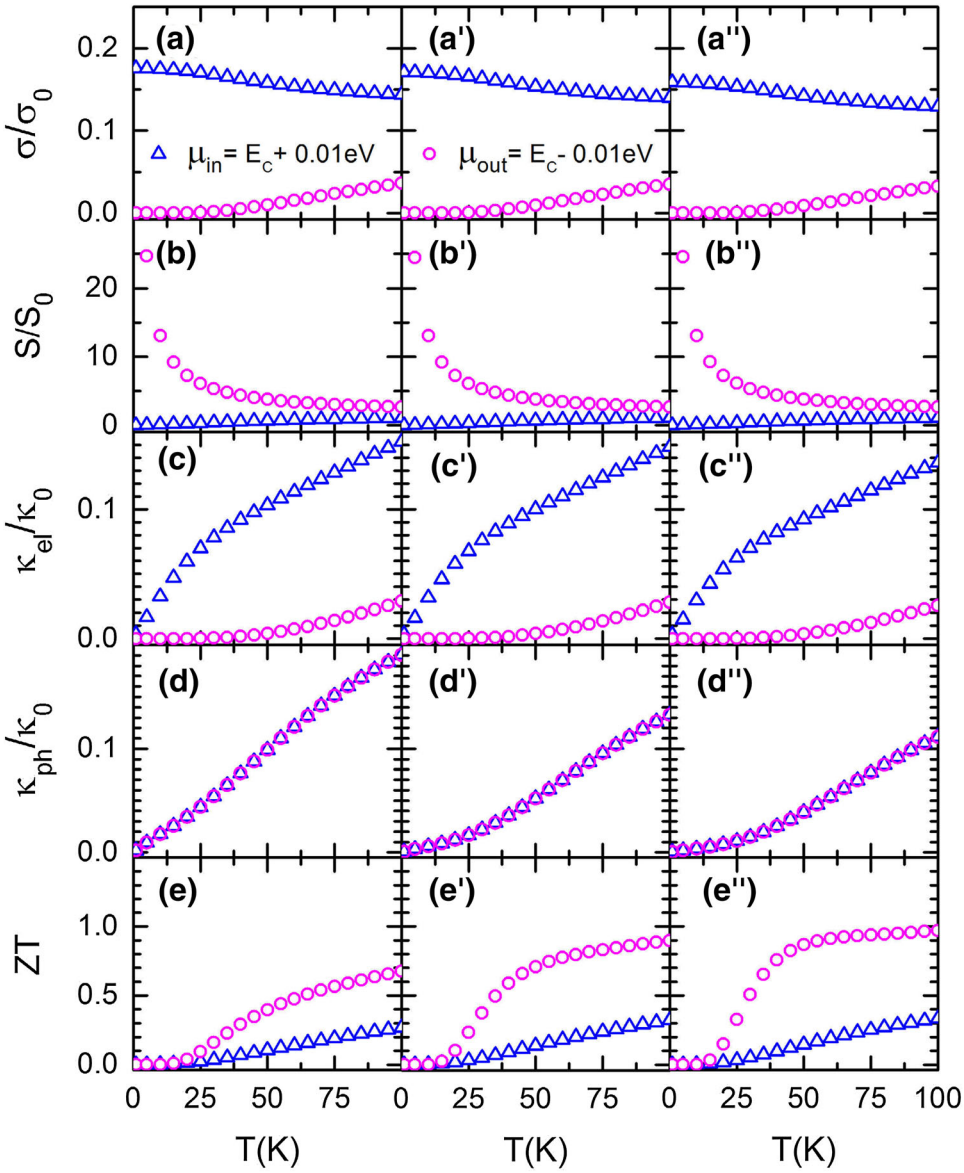

Fig. 7. Temperature (T) dependence of (a, a′, a″) electrical conductivity (σ), (b, b′, b″) Seebeck coefficient (S), thermal conductivities by (c, c′, c″) electrons (κ_{el}) and (d, d′, d″) phonons (κ_{ph}), and (e, e′, e″) figure-of-merit (ZT) for periodically segmented nanobelt and nanowires with cross-sections of (a–e) 7 × 1, (a′–e′) 7 × 3, and (a″–e″) 7 × 5 atoms.

systems and they are the hopping integral (t), atomic mass (M), central (α) and non-central (β) restoring force constants. Actually, the results only depend on two normalized ones $\hbar\omega_\alpha/|t|$ and $\hbar\omega_\beta/|t|$, where $\omega_\alpha = \sqrt{\alpha/M}$ and $\omega_\beta = \sqrt{\beta/M}$. In Fig. 10, the room-temperature (T = 300 K) thermoelectric ZT is plotted as a function of these normalized parameters for t_A/t_B = 1, 0.5, and 0.3. In the last two cases, quasiperiodically segmented nanowires with cross-section of 7 × 5 atoms are considered, as in Fig. 8. Notice a general enhancement of ZT in Fig. 10 with the quasiperiodicity strength, i.e., ZT grows when the ratio t_A/t_B moves away from the periodic case with t_A/t_B = 1, and a similar dependence of ZT on $\hbar\omega_\alpha/|t|$ and $\hbar\omega_\beta/|t|$ for the three analyzed cases. Observe also the existence of two maximums of ZT located at $\hbar\omega_\alpha \approx \hbar\omega_\beta \to 0$ and at $\hbar\omega_\alpha \approx \hbar\omega_\beta \approx 0.1|t|$ for each value of t_A/t_B, where the first one is due to the vanish of lattice thermal conductivity. The second maximum of ZT at $\hbar\omega_\alpha \approx \hbar\omega_\beta \approx 0.1|t|$ is originated from the increase of the vibrational band width when $\hbar\omega_\alpha$ and $\hbar\omega_\beta$ grow, whose phononic $\mathrm{DOS}(\omega^2)$ and $\mathrm{Tr}\left\{A_x\tilde{G}_{ph}(\omega^2)A_x\tilde{G}_{ph}(\omega^2)\right\}_l$ for the periodic case are similar to those shown in Fig. 1d.[22] In other words, the growth of $\hbar\omega_\alpha$ and $\hbar\omega_\beta$ leads to a

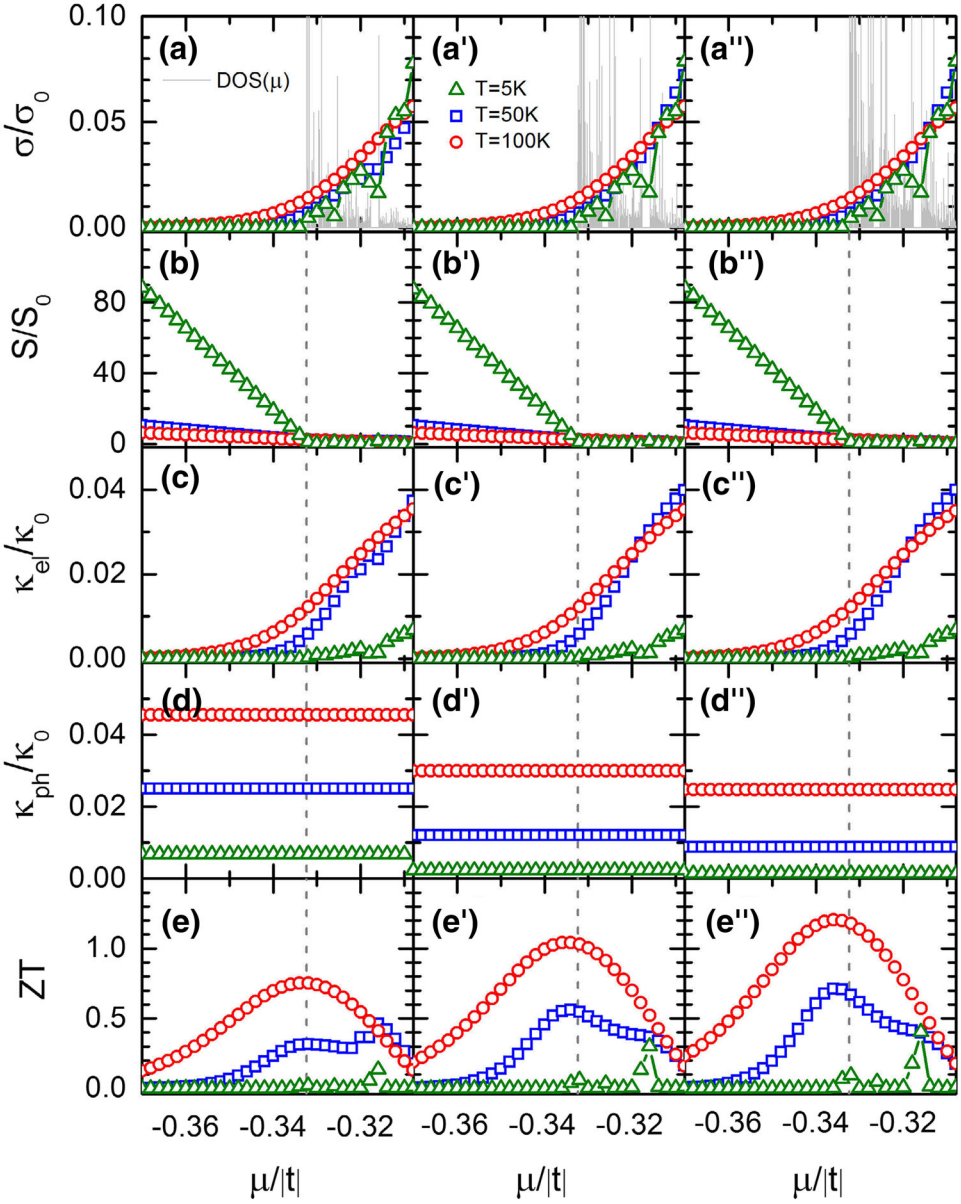

Fig. 8. (a, a′, a″). Density of states (DOS) and electrical conductivity (σ), (b, b′, b″) Seebeck coefficient (S), (c, c′, c″) thermal conductivity by electrons (κ_{el}), (d, d′, d″) thermal conductivity by phonons (κ_{ph}), and (e, e′, e″) figure-of-merit (ZT) as functions of chemical potential (μ) for quasiperiodically segmented nanobelts and nanowires with inhomogeneous cross-sections of (a–e) 7 × 1, (a′–e′) 7 × 3, and (a″–e″) 7 × 5 atoms.

shift of the maximum of both phononic DOS and $\mathrm{Tr}\left\{A_x\tilde{G}_{ph}(\omega^2)A_x\tilde{G}_{ph}(\omega^2)\right\}_l$ toward high frequency and then, for a fixed temperature the Bose–Einstein distribution in Eq. 6 will cover a smaller portion of three-dimensional phonon band. In consequence, a minor lattice thermal conductivity and a larger ZT.

Moreover, Fig. 10 shows an asymmetrical dependence of ZT on $\hbar\omega_\alpha$ and on $\hbar\omega_\beta$, since for both longitudinal and transversal vibration modes the non-central first-neighbor interactions (β) has a double contribution to the lattice thermal conductivity than the central one (α) within the Born model. It would be worth stressing that the results of ZT presented in the previous sections correspond to two specific points of $\hbar\omega_\alpha = 0.03|t|$ and $\hbar\omega_\beta = 0.0134|t|$ on the surfaces of t_A/t_B = 1 and t_A/t_B = 0.3 in Fig. 10. Hence, the enhancement of ZT through the quasiperiodicity seems to be general and independent of the Hamiltonian parameters chosen.

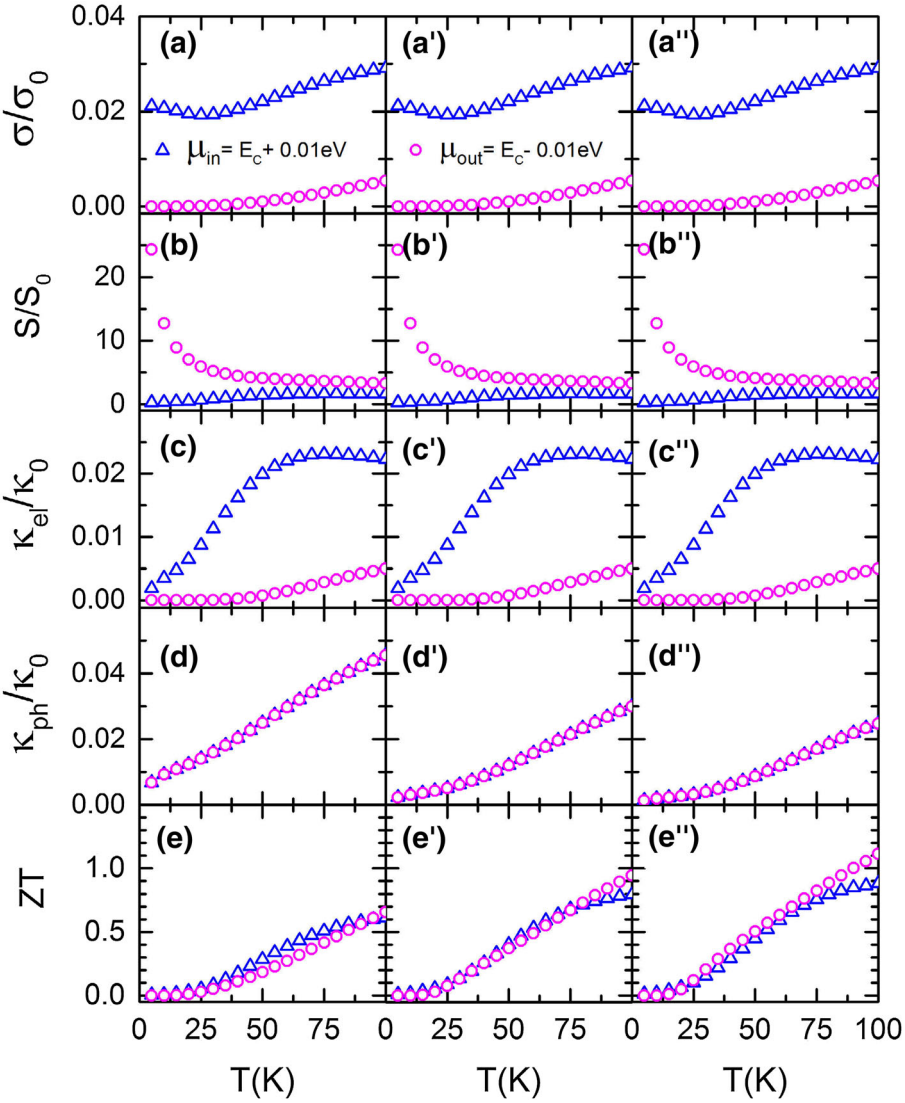

Fig. 9. Temperature (T) dependence of (a, a′, a″) electrical conductivity (σ), (b, b′, b″) Seebeck coefficient (S), (c, c′, c″) thermal conductivity by electrons (κ_{el}), (d, d′, d″) thermal conductivity by phonons (κ_{ph}), and (e, e′, e″) figure-of-merit (ZT) for quasiperiodically segmented nanobelts and nanowires with inhomogeneous cross-sections of (a–e) 7 × 1, (a′–e′) 7 × 3, and (a″–e″) 7 × 5 atoms.

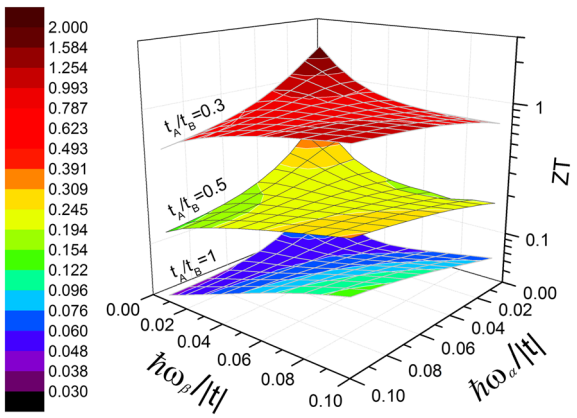

Fig. 10. Thermoelectric figure-of-merit (ZT) at 300 K as a function of normalized Hamiltonian parameters $\hbar\omega_\alpha/|t|$ and $\hbar\omega_\beta/|t|$, for a periodic nanowire with $t_A/t_B = 1$ and quasiperiodically segmented nanowires with $t_A/t_B = 0.5$ and 0.3. All these nanowires have a cross-section of 7 × 5 atoms, as in Fig. 8.

CONCLUSIONS

The effects of structural inhomogeneity on the thermoelectric properties of nanobelt and nanowires with macroscopic length are analyzed by means of a real-space renormalization plus convolution method. The results reveal a clear increase of the thermoelectric figure-of-merit (ZT) when the segmentation is introduced, in accordance with experimental data.[10] In fact, the quasiperiodicity significantly diminishes the thermal conduction of long wavelength acoustic phonons, which are responsible of the phononic conductivity at low temperature, and it is not easy to block their transmission since they do not feel local defects nor impurities. Contrary to periodic nanowires, there is no reduction of ZT when the cross-section area grows. In summary, the results of this work

suggest the possibility of optimizing the thermoelectricity through the inhomogeneity under design.

This analysis was carried out by means of semiempirical models applied to cubically structured nanowires with a specific set of parameters. However, its main result of the possibility to improve ZT by introducing long-range inhomogeneity into nanowires could not depend on the parameters chosen as shown in "Analysis of Parameter Dependence", and it would be useful in the design and fabrication of efficient thermoelectric devices, as suggested by the results of $M_2O_3(ZnO)_n$ (M = In, Ga, Fe) segmented nanowires.[10]

ACKNOWLEDGEMENTS

This work has been partially supported by Consejo Nacional de Ciencia y Tecnología de México, Project 252943, and by Programa de Apoyo a Proyectos de Investigación e Innovación Tecnológica of Universidad Nacional Autónoma de México (UNAM) through Projects IN113714 and IN114916. Computations were performed at Miztli of Dirección General de Cómputo y de Tecnologías de Información y Comunicación of UNAM, where technical assistance of Silvia E. Frausto del Río and José Luis Gordillo is fully appreciated.

REFERENCES

1. T.M. Tritt, eds., *Thermal Conductivity—Theory, Properties and Applications* (New York: Kluwer Academic-Plenum, 2004), p. 3.
2. J. Kim, J.H. Bahk, J. Hwang, H. Kim, H. Park, and W. Kim, *Phys. Status Solidi RRL* 7, 767 (2013).
3. G.J. Snyder and E.S. Toberer, *Nat. Mater.* 7, 105 (2008).
4. P. Mensch, S. Karg, V. Schmidt, B. Gotsmann, H. Schmid, and H. Riel, *Appl. Phys. Lett.* 106, 093101 (2015).
5. S. Bäßler, T. Böhnert, J. Gooth, C. Schumacher, E. Pippel, and K. Nielsch, *Nanotechnology* 24, 495402 (2013).
6. Z.M. Gibbs, H.-S. Kim, H. Wang, and J. Snyder, *Appl. Phys. Lett.* 106, 022112 (2015).
7. J.E. Cornett and O. Rabin, *Phys. Rev. B* 84, 205410 (2011).
8. J. Kim, S. Lee, Y. Brovman, P. Kim, and W. Lee, *Nanoscale* 7, 5053 (2015).
9. J. Kang, W. Shim, S. Lee, J.W. Roh, J.S. Noh, P.W. Voorhees, and W. Lee, *J. Mater. Chem. A* 1, 2395 (2013).
10. S.C. Andrews, M.A. Fardy, M.C. Moore, S. Aloni, M. Zhang, V. Radmilovic, and P. Yang, *Chem. Sci.* 2, 706 (2011).
11. A. Süto, *J. Stat. Phys.* 56, 525 (1989).
12. M. Kohmoto and B. Sutherland, *Phys. Rev. B* 35, 1020 (1987).
13. P.Y. Yu and M. Cardona, *Fundamentals of Semiconductors Physics and Materials Properties*, 4th ed. (Berlin: Springer, 2010), p. 83.
14. C. Wang and R.A. Barrio, *Phys. Rev. Lett.* 61, 191 (1988).
15. P. Alfaro, R. Cisneros, M. Bizarro, M. Cruz-Irisson, and C. Wang, *Nanoscale* 3, 1246 (2011).
16. T. Markussen, *Nano Lett.* 12, 4698 (2012).
17. B. Kramer and A. MacKinon, *Rep. Prog. Phys.* 56, 1469 (1993).
18. E.N. Economou, *Green's Functions in Quantum Physics*, 3rd ed. (Berlin: Springer, 2006), p. 6.
19. J.K. Flicker and P.L. Leath, *Phys. Rev. B* 7, 2296 (1973).
20. R.J. Elliott, J.A. Krumhansl, and P.L. Leath, *Rev. Mod. Phys.* 46, 465 (1974).
21. V. Sánchez and C. Wang, *Phys. Rev. B* 70, 144207 (2004).
22. C. Wang, F. Salazar, and V. Sánchez, *Nano Lett.* 8, 4205 (2008).
23. A.P. Sutton, *Electronic Structure of Materials* (Oxford: Oxford University Press, 1993), p. 109.
24. C. Wang, C. Ramírez, F. Sánchez, and V. Sánchez, *Phys. Status Solidi B* 252, 1370 (2015).